ARTICLE

Experimental and Theoretical Study on Pyrolysis of Isopsoralen

Jiu-zhong Yang[a], Feng Zhang[a], Liang-yuan Jia[a], Li-dong Zhang[a*], Fei Qi[a], Hai-yan Fan[b], Ji-bao Cai[b*]

a. National Synchrotron Radiation Laboratory, University of Science and Technology of China, Hefei 230029, China
b. Center of R&D, China Tobacco Jiangxi Industrial Co. Ltd., Nanchang 330096, China

(Dated: Received on January 17, 2012; Accepted on March 23, 2012)

The pyrolysis of isopsoralen was studied by synchrotron vacuum ultraviolet photoionization mass spectrometry at low pressure. The pyrolysis products were detected at different photon energies, the ratios of products to precursor were measured at various pyrolysis temperatures. The experimental results demonstrate that the main pyrolysis products are primary CO and sequential CO elimination products ($C_{10}H_6O_2$ and C_9H_6O). The decomposition channels of isopsoralen were also studied by the density functional theory, then rate constants for competing pathways were calculated by the transition state theory. The dominant decomposition channels of isopsoralen and the molecular structures for corresponding products were identified by combined experimental and theoretical studies.

Key words: Isopsoralen, Pyrolysis, Synchrotron vacuum ultraviolet photoionization mass spectrometry, Density functional theory, Transition state theory

I. INTRODUCTION

Psoralen and its isomer-isopsoralen ($C_{11}H_6O_3$) are major components of psoralea corylifolia, a Chinese medicinal herb, which has been widely used for photochemotherapeutic treatments due to its photosensitising effects [1−5]. The photochemical characteristic of psoralen and isopsoralen has been extensively studied [6−9]. However, there are few studies on the pyrolysis process, *e.g.* the thermal decomposition. Besides as medicine, psoralen and isopsoralen are also used as tobacco flavor additives. Understanding the pyrolysis products of psoralen and isopsoralen during smoking requires reliable measurements on its pyrolysis process.

The importance of studying isolated pyrolysis for establishing the relationship between tobacco constituents and smoke products has been reviewed by researchers [10−14]. Pyrolysis gas chromatography/mass spectrometry (Py-GC/MS) is the most often used technique in tobacco chemistry due to its high sensitivity, high mass accuracy and simplicity [11, 12, 15]. However, Py-GC/MS suffers from the disadvantage that some pyrolysis products may be lost because they are too polar and/or involatile to chromatograph [16]. Recently, we have combined experimental and theoretical studies to investigate the pyrolysis process of psoralen molecule [17]. In this present work, we investigated the pyrolysis processes of isopsoralen by synchrotron vacuum ultraviolet photoionization mass spectrometry (SVUV-PIMS) combined with molecular-beam sampling [18]. This soft ionization technique provides *in situ* and fragmentation-controllable detection of pyrolysis products [19−23].

Nowadays, theoretical calculation has performed as a very useful tool for validating and explaining pyrolysis experimental results, especially with the development of density functional theory [24, 25]. In this work, the hybrid density functional-B3LYP was used to calculate the decomposition pathways of isopsoralen. B3LYP is the most successful functional in past years, which also served as a good functional for heterocyclic aromatic compounds compared with experiments [26, 27]. Dominant decomposition channels and their products can be identified by calculating potential energy profiles. We also calculated the rate constants of the two competing decomposition channels with similar barrier heights by the conventional transition state theory (TST) [28], which helped us to ultimately verify the molecular structure of the primary pyrolysis products of isopsoralen.

II. EXPERIMENTAL AND THEORETICAL METHODS

A. Experimental methods

The experiments were performed at the National Synchrotron Radiation Laboratory (NSRL) in Hefei, China. SVUV light and experiment apparatus have been described in detail elsewhere [18]. Briefly, the experimental apparatus consists of a pyrolysis chamber with

*Authors to whom correspondence should be addressed. E-mail: zld@ustc.edu.cn, jbcai@ustc.edu.cn

a PYR-2A pyrolyzer (Shimadzu, Kyoto, Japan) and a photoionization chamber including a homemade reflectron time-of-flight mass spectrometer (RTOF-MS). The temperature of the pyrolyzer could be measured by a K-type thermocouple and controlled by a temperature controller (SKY Technology Development Co., Ltd., Shenyang, China). Argon, as the carrier gas, was used to bring the gas phase products to photoionization chamber with a flow rate of 20.00 standard cubic centimeters per minute (SCCM), which was controlled by a mass flow controller (MKS Instruments, Andover, MA, USA). The gaseous pyrolysis products were brought into the photoionization region through a nickel skimmer with a 1.5-mm-diameter orifice in the tip and then ionized by SVUV light.

The sample of isopsoralen was purchased from Aladdin Reagent Inc. (Shanghai, China) with a purity over 98%. The feedstock weights for each measurement in the pyrolysis of psoralen and isopsoralen were 1.0 and 2.0±0.2 mg, respectively.

During the experiment, the temperature of the pyrolyzer increased from 373 K to 973 K with a step of 50 K. At each temperature, mass spectra were obtained at seven photon energies including 14.5, 12.0, 11.5, 11.0, 10.5, 10.0, and 9.5 eV. The signal ratio profiles versus different photon energies and temperatures can estimate the photoionization efficiency (PIE) of products and monitor the pyrolysis process, respectively.

B. Theoretical methods

The lowest energy geometry of isopsoralen was optimized at the B3LYP/6-31++G(d,p) level. Then possible decomposition channels of isopsoralen were studied by step-wised optimization, while corresponding transition states and products were fully optimized at the same level. Harmonic frequencies were computed to verify the nature of all stationary points and evaluate the zero-point energy correction. In order to ensure that the optimized transition states connect the desired reactants and products, the intrinsic reaction coordinate (IRC) calculations were employed for each transition state geometry [29]. All above calculations were carried out with Gaussian 03 program package [30].

In addition, the conventional TST was used to calculate the high pressure limit rate constants of competing decomposition channels. The rate constant k is given by Eq.(1) [28]

$$k_{\mathrm{TST}}(T) = \sigma \frac{k_{\mathrm{B}}T}{h} \frac{Q_{\mathrm{TS}}(T)}{Q_{\mathrm{R}}(T)} \exp\left(-\frac{E_{\mathrm{a}}}{k_{\mathrm{B}}T}\right) \qquad (1)$$

where T is the temperature, σ is the reaction symmetry number, k_{B} is Boltzmann's constant, h is Plank's constant, $Q_{\mathrm{TS}}(T)$ and $Q_{\mathrm{R}}(T)$ are the semi-classical partition functions for the transition state and reactant, respectively, E_{a} refers to the activation energy. The rate constant calculated by Eq.(1) requires information of barrier heights, rotational and vibrational energy levels of the reactant and transition state, which are all obtained by the above quantum chemical calculations. The rate constant calculation was performed using ChemRate program [31].

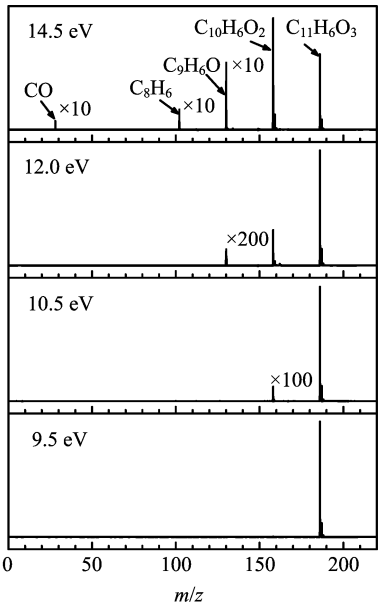

FIG. 1 Photoionization mass spectra of isopsoralen at a temperature of 973 K and photon energies of 14.5, 12.0, 10.5, and 9.5 eV. "×number" represent that they have been multiplied with corresponding times.

III. RESULTS AND DISCUSSION

Figure 1 shows the photoionization mass spectra of isopsoralen pyrolysis measured at 973 K with different photon energies including 14.5, 12.0, 10.5, and 9.5 eV. Mass peaks at m/z=158, 130, 102, and 28, corresponds to $C_{10}H_6O_2$, C_9H_6O, C_8H_6, and CO, respectively. For some weak peaks, the measured intensity was multiplied by a factor of 100, 200 or 10 for distinction, as marked in Fig.1. The peak at m/z=158 was observed gradually as photon energy increases. Clearly, the primary decomposition channel of isopsoralen is CO emission. The signal of C_9H_6O (m/z=130) originates from isopsoralen losing two CO molecules. Comparing the mass spectra measured at different photon energies (see Fig.1), the peak at m/z=102 was only observed at 14.5 eV, indicating that it is the fragmentation and/or pyrolysis products of isopsoralen because the ionization energy of m/z=102 species was lower than 12.0 eV.

Figure 2 displays the normalized signal ratio profiles of $C_{10}H_6O_2/C_{11}H_6O_3$ (at 10.5 eV) and $C_9H_6O/C_{11}H_6O_3$ (at 12.0 eV). In order to minimize the fragmentation, the value of photon energy used to scan temperatures should be higher than the ionization en-

DOI:10.1088/1674-0068/25/03/249-253

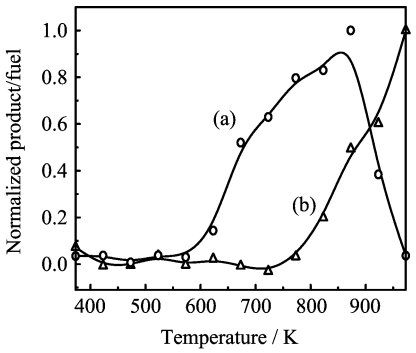

FIG. 2 The normalized signal ratio profiles of (a) C_9H_6O to $C_{11}H_6O_3$ and (b) $C_{10}H_6O_2$ to $C_{11}H_6O_3$ versus the temperatures.

ergy threshold (PIE). As shown in Fig.1, the C_9H_6O begins to appear at the photon energy of 12 eV without fragmentation, while the same photon energy isn't suitable to the $C_{10}H_6O_2$ because it likely leads to further fragmentation. Therefore, the photon energy of 10.5 eV is used for $C_{10}H_6O_2$. The formation temperatures (T_F) of two species can be seen from Fig.2 directly. The $C_{10}H_6O_2$ first forms at around 570 K by eliminating CO molecule from isopsoralen, then further emits a CO molecule forming C_9H_6O whose T_F is about 720 K. From Fig.1 and Fig.2, we conclude that the thermal decomposition of isopsoralen mainly involve primary and secondary CO elimination reactions.

The experiments provide the information of the molecular formula of primary decomposition products and their formation temperatures during pyrolysis process. Although it's possible to estimate the molecular structures from above information, what reactions happen and how they happen is still unknown. For this reason, we employed quantum chemical calculations to explore possible reaction pathways in isopsoralen thermal decomposition, and more importantly to identify the molecular structures for the pyrolysis products detected by the experiments. Figure 3 presents the primary and secondary decomposition channels of isopsoralen (labeled as RC) calculated at the B3LYP/6-31++G(d, p) level. The direct CO dissociation originating from the destruction of the carbonyl group with a barrier height of 360.23 kJ/mol results in the formation of benzodifuran compound (PC1). Subsequently, PC1 can eliminate another CO molecule to generate PC2. It appears that another decomposition reaction with a slightly high barrier (via TS4) competes with it. However we didn't observe the signal of C_8H_4O (PC3) in the experiment, implying the minor contribution of this channel. The product PC5 ($C_9H_4O_2$) is also not detected in the experiment for the high barrier. An isomerization channel is found for isopsoralen molecule, which has a quite low barrier height (281.52 kJ/mol). The isomerized product (INT2) can eliminate a CO to form $C_{10}H_6O_2$ (PC4) with a very low barrier (144.67 kJ/mol).

At this stage, we conclude that the two channels: RC→PC1+CO→PC2+2CO and RC→PC4+CO are two controlling reaction channels involved in the pyrolysis of isopsoralen, the observed signal of C_9H_6O has the structure like PC2 or its isomer, and the observed signal of $C_{10}H_6O_2$ corresponds to the mixture of PC1 and PC4. Since the highest transition states in these two channels (TS1 and TS6) have very close energies: 360.23 and 366.88 kJ/mol. It requires further kinetic studies, *e.g.* the rate constant calculations to investigate the competition between these two channels.

Figure 4 illustrates the calculated rate constants for the two competing CO decomposition channels, *e.g.* RC→PC1+CO (channel 1) and RC→PC4+CO (channel 2), in the temperature range of 300−1000 K, with Fig.4(b) showing the ratio between them. It can be seen that the direct CO dissociation channel is slightly more favored than the multi-step CO dissociation among the interested temperature range. The ratio of the rate constants of channel 1 to channel 2 varies from 12.3 to 1.9 in the temperature range of 300−1000 K. With the temperature rising, the rate constants of these two channels become much closer to each other. Therefore, the contribution of PC1 in the observed $C_{10}H_6O_2$ signal should be slightly larger than that of PC4. Combining our quantum chemical results and the rate constants calculations, we predict that the observed peak of m/z=158 in mass spectra corresponds to the two isomers of $C_{10}H_6O_2$ with the structures like PC1 and PC4 shown in Fig.3. Note that PC4 can also eliminate a CO molecule to form a product has the formula of C_9H_6O, which is calculated in this work for simplicity. The peak at m/z=130 corresponds to the structure of PC2 or its isomer, *e.g.* the product of PC4 emitting a CO molecule.

IV. CONCLUSION

The pyrolysis of isopsoralen at low pressure has been investigated by SVUV-PIMS technique. The mass spectra were recorded as a function of photon energy and temperature. The experimental results demonstrate that the main pyrolysis products are CO and two sequential CO elimination products ($C_{10}H_6O_2$ and C_9H_6O). The formation temperatures of $C_{10}H_6O_2$ and C_9H_6O are around 570 and 720 K, respectively. The potential energy profiles of isopsoralen decomposition channels were calculated by density functional theory. And the rate constants of two competing reaction channels with close barrier heights were computed by transition state theory. Our theoretical calculations help to identify the two dominant decomposition channels of isopsoralen, *e.g.* RC→PC1+CO→PC2+2CO and RC→PC4+CO. The structures of decomposition products are verified as well. This work also proposed a combined experimental and theoretical methodology to investigate the pyrolysis of a molecule including the

DOI:10.1088/1674-0068/25/03/249-253

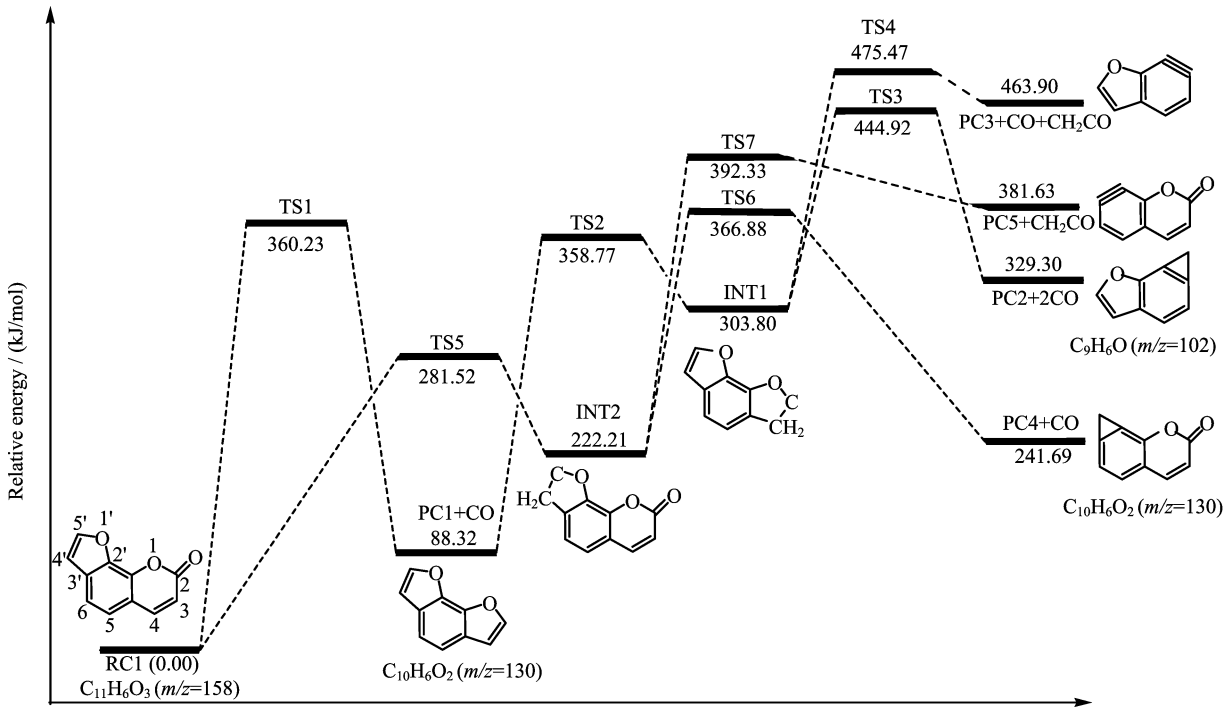

FIG. 3 The calculated decomposition pathways of isopsoralen at B3LYP/6-31++G(d,p) level. RC, TS, INT, and PC are abbreviations of reactant, transition state, intermediate, and product, respectively.

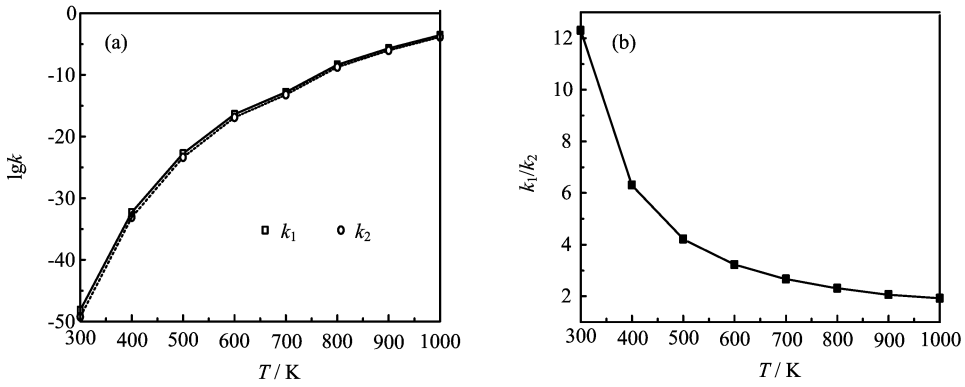

FIG. 4 (a) The calculated rate constants of the competing CO elimination channels of isopsoralen *i.e.* the channels: RC→PC1+CO (k_1) and RC→PC4+CO (k_2). (b) The ratio of k_1 to k_2 versus temperature.

chemistry happening during the process.

V. ACKNOWLEDGMENTS

We thank Dr. Yu-yang Li for the kind help in performing the experiments and writing the manuscript. The numerical calculations were supported by the Supercomputing Center of USTC.

[1] S. N. Wu, Z. H. Zhang, and J. B. Zhao, China J. Chin. Mater. Med. **23**, 303 (1998).

[2] S. Q. Mi, X. Hong, T. L. Huang, S. M. Ye, W. P. Ou, M. R. Feng, Q. W. Xu, and Q. D. Liu, Tradit. Chin. Drug Res. Clin. Pharmacol. **9**, 147 (1998).

[3] T. M. Mariano and A. M. Vetrano, Biochem. Pharmacol. **63**, 31 (2002).

[4] D. Bethea, B. Fullmer, S. Syed, G. Seltzer, J. Tian, C. Rischko, L. Gillespie, D. Brown, and F. P. Gasparro, J. Dermatol. Sci. **19**, 78 (1999).

[5] N. M. B. Abdel, U. Wollina, M. EI Okby, and S. E. Shiemy, Clin. Exp. Dermatol. **29**, 380 (2004).

[6] E. P. Jarvenpaa, M. N. Jestoi, and R. Huopalahti, Phytochem. Anal. **8**, 250 (1997).

[7] J. Llano, J. Raber, and L. A. Eriksson, J. Photochem. Photobio. A **154**, 235 (2003).

[8] J. J. Serrano-Perez, L. Serrano-Andres, and M. Merchan, Chem. Phys. **347**, 422 (2008).

DOI:10.1088/1674-0068/25/03/249-253

[9] A. Y. Potapenko, J. Photochem. Photobiol. B **9**, 1 (1991).
[10] R. R. Baker and L. L. Bishop, J. Anal. Appl. Pyrolysis **71**, 223 (2004).
[11] Z. Czégény, M. Blazsó, G. Várhegyi, J. E. C. Lou, and L. Nappi, J. Anal. Appl. Pyrolysis **85**, 47 (2009).
[12] G. Wang, Z. Hou, Y. Suan, R. Zhang, K. Xie, and R. Liu, J. Hazard. Mater. **129**, 22 (2006).
[13] T. Adam, T. Streibel, S. Mitschke, F. Mühlberger, R. R. Baker, and R. Zimmermann, J. Anal. Appl. Pyrolysis **74**, 454 (2005).
[14] R. W. Jenkins Jr. and D. D. D. D. McRae, Rec. Adv. Tob. Sci. **22**, 337 (1996).
[15] S. Wang, B. Liu, and Q. Su, J. Anal. Appl. Pyrolysis **71**, 393 (2004).
[16] F. Mellon, R. Self, and J. R. Startin, *Mass Spectrometry of Natural Substances in Food*, Cambridge: Royal Society of Chemistry, (2000).
[17] H. Fan, K. Liao, W. Hu, J. Su, Y. Tian, F. Qi, and J. Cai, Chin. J. Chin. Mater. Medica **37**, 207 (2012).
[18] J. Li, J. H. Cai, T. Yuan, H. J. Guo, and F. Qi, Rap. Commun. Mass Spectrom. **23**, 1269 (2009).
[19] Y. Y. Li and F. Qi, Acc. Chem. Res. **43**, 68 (2010).
[20] Z. Y. Zhou, H. J. Guo, and F. Qi, Trend. Anal. Chem. **30**, 1400 (2011).
[21] Y. Pan, L. D. Zhang, H. J. Guo, L. L. Deng, and F. Qi, Int. Rev. Phys. Chem. **29**, 369 (2010).
[22] K. Kohse-Hoinghaus, P. Osswald, T. A. Cool, T. Kasper, F. Qi, C. K. Westbrook, and P. R. Westmoreland, Angew. Chem. Int. Ed. **49**, 3572 (2010).
[23] C. A. Taatjes, N. Hansen, A. Mcllroy, J. A. Miller, J. P. Senosiain, S. J. Klippenstein, F. Qi, L.S. Sheng, Y. W. Zhang, T. A. Cool, J. Wang, P. R. Westmoreland, M. E. Law, T. Kasper, and K. Kohse-Hoinghaus, Science **308**, 1887 (2005).
[24] X. Hong, L. Zhang, T. Zhang, and F. Qi, J. Phys. Chem. A **113**, 5397 (2009).
[25] I. Reva, S. Breda, T. Roseiro, E. Eusebio, and R. Fausto, J. Org. Chem. **70**, 7701 (2005).
[26] A. D. Becke, J. Chem. Phys. **98**, 5648 (1993).
[27] C. T. Lee, W. T. Yang, and R. G. Parr, Phys. Rev. B **37**, 785 (1988).
[28] D. G. Truhlar, A. D. Isaacson, and B. C. Garrett, Eds., *Theory of Chemical Reaction Dynamics*, Vol. 4, Boca Raton: CRC Press, (1985).
[29] C. Gonzalez and H. B. Schlegel, J. Phys. Chem. **94**, 5523 (1990).
[30] M. J. Frisch, G. W. Trucks, H. B. Schlegel, G. E. Scuseria, M. A. Robb, J. R. Cheeseman, J. A. Montgomery Jr., T. Vreven, K. N. Kudin, J. C. Burant, J. M. Millam, S. S. Iyengar, J. Tomasi, V. Barone, B. Mennucci, M. Cossi, G. Scalmani, N. Rega, G. A. Petersson, H. Nakatsuji, M. Hada, M. Ehara, K. Toyota, R. Fukuda, J. Hasegawa,M. Ishida, T. Nakajima, Y. Honda, O. Kitao, H. Nakai, M. Klene, X. Li, J. E. Knox, H. P. Hratchian, J. B. Cross, V. Bakken, C. Adamo, J. Jaramillo, R. Gomperts, R. E. Stratmann, O. Yazyev, A. J. Austin, R. Cammi, C. Pomelli, J. W. Ochterski, P. Y. Ayala, K. Morokuma, G. A. Voth, P. Salvador, J. J. Dannenberg, V. G. Zakrzewski, S. Dapprich, A. D. Daniels, M. C. Strain, O. Farkas, D. K. Malick, A. D. Rabuck, K. Raghavachari, J. B. Foresman, J. V. Ortiz, Q. Cui, A. G. Baboul, S. Clifford, J. Cioslowski, B. B. Stefanov, G. Liu, A. Liashenko, P. Piskorz, I. Komaromi, R. L. Martin, D. J. Fox, T. Keith, M. A. Al-Laham, C. Y. Peng, A. Nanayakkara, M. Challacombe, P. M. W. Gill, B. Johnson, W. Chen, M. W. Wong, C. Gonzalez, and J. A. Pople, *Gaussian 03, Revision C.02*, Pittsburgh, PA: Gaussian, Inc., (2004).
[31] V. Mokrushin, V. Bedanov, W. Tsang, M. Zachariah, and V. Knyazev. ChemRate program, version 1.5.2, National Institute of Standards and Testing, Gaithersburg, MD, (2006).

DOI:10.1088/1674-0068/25/03/249-253